

Kinetics of HL-60 Cell Entry to Apoptosis During Treatment With TNF- α or Camptothecin Assayed by the Stathmo-Apoptosis Method

Piotr Smolewski,^{1,2} Jerzy Grabarek,^{1,3} Brian W. Lee,⁴ Gary L. Johnson,⁴ and Zbigniew Darzynkiewicz^{1*}

¹Brander Cancer Research Institute, New York Medical College, Valhalla, New York

²Department of Hematology, Medical University, Lodz, Poland

³Department of Pathology, Pomeranian School of Medicine, Szczecin, Poland

⁴Immunochemistry Technologies, Bloomington, Minnesota

Received 4 August 2001; Revision received 8 December 2001; Accepted 12 December 2001

Background: Duration of apoptosis, from onset to final disintegration of the cell, is often short and variable. The apoptotic index (AI), as a snapshot of a transient event of variable length, does not truly represent incidence of apoptosis in the studied cell population. We recently proposed to estimate the cumulative apoptotic index (CAI) by inducing stathmo-apoptosis. A fluorescent inhibitor of caspases (FLICA) FAM-VAD-FMK is used to arrest the process of apoptosis and thereby prevent cell disintegration. Simultaneously, the arrested/apoptotic cells become FLICA-labeled. In the present study, this approach was applied to measure kinetics of HL-60 cell entrance into apoptosis induced via cell surface death receptor or a mitochondria-initiated pathway.

Materials and Methods: Cultures of HL-60 cells were treated with either TNF- α or camptothecin (CPT) in the absence or constant presence of 10–50 μ M FLICA. The CAI was measured at different time points for up to 48 h by flow cytometry. Bivariate analysis of DNA content and cell labeling with FLICA was used to correlate apoptosis with the cell-cycle position.

Results: Selective loss of apoptotic cells seen in HL-60 cell cultures exposed to either TNF- α or CPT alone was prevented in cultures containing FLICA. Addition of FLICA alone had no effect on cell viability. The percentage of FLICA-labeled cells was plotted as a function of time after

addition of TNF- α or CPT. The rate of cell entry to apoptosis was subsequently estimated from the slopes of the stathmo-apoptotic plot. The slopes revealed that the TNF- α or CPT-treated cells asynchronously underwent apoptosis with a stochastic-like kinetics and at two different rates. About 50% of cells in the TNF- α -treated cultures underwent apoptosis during the initial 6 h at a rate of \sim 8% of cells per hour; the remaining cells were undergoing apoptosis at a rate of \sim 2.5% of cells per hour for up to 24 h. Also, about 50% of the CPT-treated cells, predominantly those in S phase of the cell cycle, underwent apoptosis within the initial 8 h of CPT exposure, at a rate of \sim 7% of cells per hour. Remaining cells were undergoing apoptosis at a rate of \sim 1% of cells per hour during up to 48 h exposure to CPT. Spontaneous apoptosis in the untreated cultures occurred at a rate of 0.2% of cells per hour.

Conclusions: This approach provides a means for measuring the kinetics of cell entrance to apoptosis (caspase activation) in large populations of cells in relation to the cell-cycle position. Cytometry 47:143–149, 2002.

© 2002 Wiley-Liss, Inc.

Key terms: FLICA; caspases; cell necrobiology; cell cycle; S phase; cumulative apoptotic index; stathmo-apoptosis

Apoptosis plays a critical role in the etiology, pathogenesis, and therapy of a variety of diseases (1–4). The estimation of the incidence of apoptosis, therefore, is of importance in many disciplines of biology and medicine. Cytometric methods of apoptosis can provide a “snapshot” estimate of the percentage or fraction of apoptotic cells (apoptotic index, AI) at a particular time-point (5–7). However, because apoptosis is a transient, kinetic event, such estimates can be inaccurate. The entire apoptotic process, from onset to ultimate cell disintegration, when

the cell is no longer detectable, is often short and of variable duration (1–3,8). The time-window during which the individual cell displays its characteristic apoptotic

Grant sponsor: NCI; Grant number: CA 28704; Grant sponsor: Chemotherapy Foundation; Grant sponsor: “This Close” Foundation for Cancer Research.

*Correspondence to: Dr. Z. Darzynkiewicz, Brander Cancer Research Institute at NYMC, 19 Bradhurst Ave., Suite 2400, Hawthorne, NY 10532.
E-mail: darzynk@nymc.edu

feature (marker) is dependent on type of assay, cell lineage, and nature of the apoptosis-inducing agent. The longer the duration of time-window through which a particular assay recognizes the apoptotic cell, the higher the AI is determined in the same cell population (9). In addition, some inducers of apoptosis or factors in the cellular environment may alter the duration of the apoptotic process, e.g., by affecting formation and/or shedding of apoptotic bodies, proteolysis, or DNA degradation. When the duration of apoptosis is shortened, the AI is diminished. Conversely, prolongation of the apoptotic process results in an increase in AI, even if the incidence rate of apoptosis induction remains unchanged (9).

The duration of apoptosis is also different in different cell types and tissues, as well as *in vivo* and *in vitro*. Cells of hematopoietic tumor lines (e.g., Jurkat, HL-60, U937), when triggered by internal stress or cell surface death ligands, progress through the entire process of apoptosis rapidly, often disintegrating within 4–6 h after the treatment. The same treatment of cells of epithelial or fibroblast lineage often triggers apoptosis with a 24-h delay, and the apoptotic process is of much longer duration (10). It should be noted that duration of apoptosis *in vivo* appears to be short, as reflected by the fact that in tissue, under conditions of homeostasis, AI values often approximate the mitotic index (1,2,8). Because mitosis lasts ~1 h, apoptosis must be of comparable duration.

To obtain a more accurate assessment of the incidence of apoptosis, we propose to estimate the cumulative apoptotic index (CAI) (11). The fluorescent inhibitor of caspases (FLICA) FAM-VAD-FMK (12,13) is used in this approach to arrest cells in apoptosis, thereby preventing their disintegration and loss from analysis (11). Because the arrested (apoptotic) cells become fluorochrome-labeled, they could easily be identified by fluorescence microscopy, as well as flow or laser-scanning cytometry. We also propose to define the event in which cells are arrested in apoptosis as *stathmo-apoptosis* (11). This process is analogous to stathmo-kinesis, the assay that is commonly used to estimate cell birth rate from a slope of the plot representing mitotic cell accumulation during their arrest by a mitotic poison (14–16).

In the present study, this method was used to measure the kinetics of HL-60 cell entrance to apoptosis (*cell death rate*) after induction either along cell surface death receptor (TNF- α)- or DNA-damage mitochondrial-apoptotic pathways (17,18). Different concentrations of FAM-VAD-FMK were tested to find optimal conditions, which fully halt the process of apoptosis and at the same time, provide adequate cell labeling. Additionally, the method was extended to reveal a relationship between cell position in the cell cycle and kinetics of entrance to apoptosis.

MATERIALS AND METHODS

Cells

Human promyelocytic leukemic HL-60 cells obtained from the American Type Culture Collection (ATCC; Rockville, MD) were cultured in 25 ml (12.5 cm²) Falcon flasks

(Becton Dickinson Co., Franklin Lakes, NJ) in RPMI-1640 supplemented with 10% fetal calf serum, 100 units/ml penicillin, 100 mg/ml streptomycin, and 2 mM L-glutamine. Cell cultures were maintained in a humidified incubator at 37.5°C in 5% CO₂. Cell concentrations at the onset of these experiments were less than 5×10^5 cells per ml. Cell growth rate at this concentration and time-point was exponential and asynchronous. All media, supplements, and antibiotics were obtained from Life Technologies (Grand Island, NY).

FLICA

FAM-VAD-FMK was obtained from Intergen Co. (Purchase, NY). This inhibitor, which is commercially available as a component of the CaspaTag™ Fluorescein Caspase Activity Kit, was dissolved in dimethylsulfoxide (Sigma Chemical Co., St. Louis, MO) as specified in the protocol provided with the kit, to obtain a 150 \times concentrated (stock) solution. Aliquots of this solution were stored at –20°C in the dark. The solution of FAM-VAD-FMK was mixed with a solution of the unlabeled inhibitor z-VAD-FMK (R&D Systems, Inc., Minneapolis, MN) in a 1:4 molar ratio. This mixture was added to the cell cultures to obtain a 20–50- μ M final concentration of inhibitor. Other cultures were treated with 10 μ M FAM-VAD-FMK that did not contain the z-VAD-FMK inhibitor. Other details are presented in the figure legends.

Cell Staining and Fluorescence Measurement

The cells from 25-ml Falcon flasks were transferred into two parallel sets of 96-well plate cultures containing a 300- μ l cell suspension per well (Corning Glass Works, Corning, NY). Plates were treated at time 0 with either a combination of 0.3 nM TNF- α and 5 μ M cycloheximide (CHX; both from Sigma) or with 0.15 μ M DNA topoisomerase I inhibitor camptothecin (CPT; Sigma) as described before (12,13) for different periods of time, as specified in the figure legends. FAM-VAD-FMK was introduced into one set of cultures at a final concentration range between 10–50 μ M, as indicated in the figure legends. The other set of cultures was treated with FAM-VAD-FMK only during the final hour of incubation. All cells were then washed 2 \times (2 ml, 200g, 5 min) with the “wash buffer” (component of the CaspaTag™ kit, Intergen), diluted as recommended in the kit protocol. Cell pellets were then resuspended in 1 ml of the “wash buffer” containing 1 μ g of propidium iodide (PI; Molecular Probes, Inc., Eugene, OR). The samples were placed on ice, and cell fluorescence was measured during the next 15 min by the FAC-Scan (Becton Dickinson, San Jose, CA) flow cytometer, using the standard green (FL1) and red (FL3) emission filters. After washing, some samples were fixed for 15 min in PBS containing 1% v/v methanol-free formaldehyde. These samples were subsequently postfixxed in 70% ethanol, followed by another wash in PBS. Fixed cells were then stained with PI (10 μ g/ml in PBS) in the presence of 100 μ g/ml of RNase A (Sigma), as described previously (13). Red and green fluorescence was measured by FAC-Scan as described above. Still other samples after postfix-

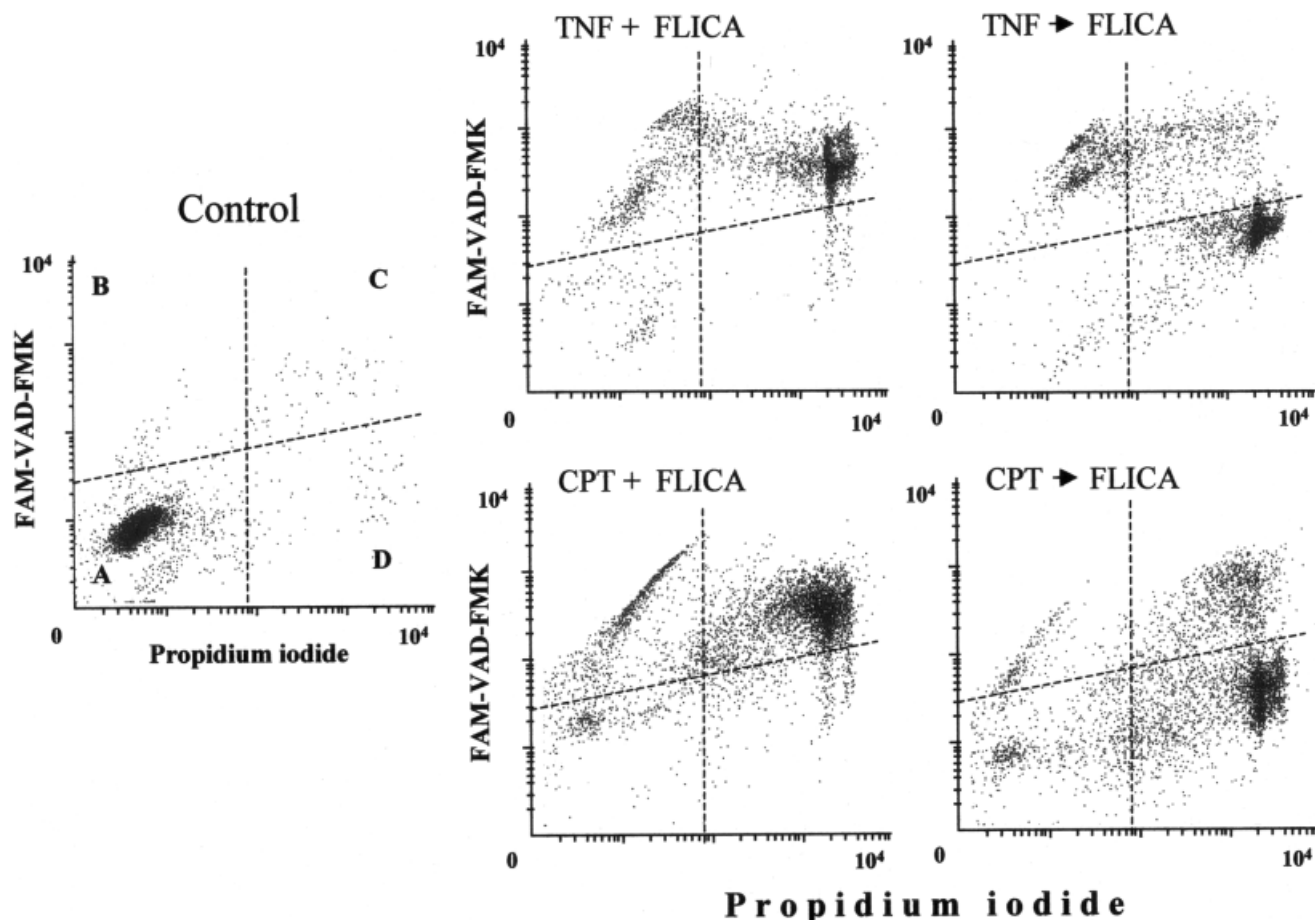


FIG. 1. Dual-fluorescence staining of HL-60 cells treated with $\text{TNF-}\alpha$ + CHX or CPT or untreated (control) in the continuous presence or absence of FAM-VAD-FMK, using FAM-VAD-FMK (FLICA) and propidium iodide (PI) reagents. Apoptosis was induced in cultures by administering $\text{TNF-}\alpha$ + CHX (top) or CPT (bottom) at time 0. In one set of cultures, FAM-VAD-FMK ($20 \mu\text{M}$) was included in the media from the outset, along with $\text{TNF-}\alpha$ + CHX or CPT ($\text{TNF-}\alpha$ + FLICA, CPT + FLICA). Twenty micromoles of FAM-VAD-FMK were added to a second set of $\text{TNF-}\alpha$ + CHX- or CPT-treated cultures 1 h prior to culture termination ($\text{TNF-}\alpha \rightarrow \text{FLICA}$, CPT $\rightarrow \text{FLICA}$). $\text{TNF-}\alpha$ and CPT-treated cultures were maintained for 24 and 48 h, respectively. Cells from all cultures were supravivally stained with PI ($1 \mu\text{g/ml}$), 5 min prior to fluorescence measurement. Green (FAM-VAD-FMK) and red (PI) cellular fluorescence was measured by flow cytometry. Four cell subpopulations (A–D) can be identified on these scattergrams, differing in their capability to bind FAM-VAD-FMK and PI, as described in the text. They represent the progressive stages of apoptosis, starting with caspase activation (B), loss of plasma membrane ability to exclude PI (C), and loss of caspase reactivity with FAM-VAD-FMK (D). Note that in cultures continuously treated with FLICA, very few cells underwent the transition from C to D.

ation in 70% ethanol were washed in PBS and stained with $2 \mu\text{g/ml}$ of 7-aminoactinomycin D (7-AAD, Molecular Probes), and their green and far red fluorescence was measured with a laser scanning cytometer (CompuCyte, Cambridge, MA), as described (13). Other details are provided in the figure legends.

RESULTS

The bivariate distributions (scatterplots) of green and red fluorescence intensity levels, from cells “supravivally” stained with FAM-VAD-FMK (FLICA) and PI, revealed the presence of four distinct subpopulations which differed in fluorochrome binding (Fig. 1). Nonapoptotic cells, which predominated in the control untreated samples, showed neither FLICA nor PI fluorescence (FLICA $^-$ /PI $^-$; subpopulation A). Cells that made up the second subpopulation (B) were FLICA $^+$ /PI $^-$. There were two subpopula-

tions of PI-stained cells: one comprised the cells that were FLICA-positive (subpopulation C; FLICA $^+$ /PI $^+$), and the other, of FLICA-negative cells (subpopulation D; FLICA $^-$ /PI $^+$). The B, C, and D subpopulations represented the consecutive stages of apoptosis: the initial activation phase, when caspases become enzymatically activated but the plasma membrane was still able to exclude PI (FLICA $^+$ /PI $^-$), followed by loss of the cell’s ability to exclude PI (FLICA $^+$ /PI $^+$) and by loss of its ability to bind FLICA (FLICA $^-$ /PI $^+$). Because the late phase of apoptosis during which the plasma membrane becomes permeable to cationic dyes such as PI or Trypan blue has been defined as the “necrotic stage” of apoptosis (2), the FLICA $^+$ /PI $^+$ and FLICA $^-$ /PI $^+$ cells thus represent two consecutive phases of the “necrotic stage.”

The distributions shown in Figure 1 represent two parallel sets of cultures: (1) the cultures that contained FLICA

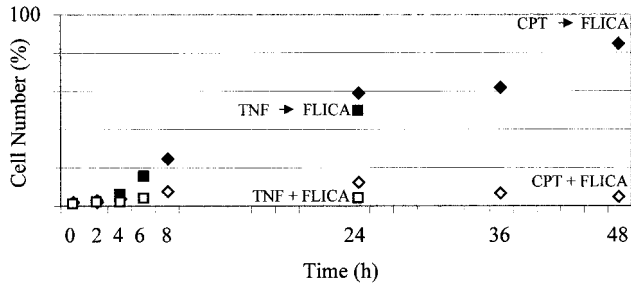


Fig. 2. Percent of FLICA⁻/PI⁺ cells (subpopulation D, see Fig. 1) in cultures of HL-60 cells treated with TNF- α + CHX or CPT that either had FAM-VAD-FMK included at time 0 (TNF + FLICA; CPT + FLICA, open symbols) or only during the final hour (TNF → FLICA; CPT → FLICA, solid symbols) prior to culture termination.

throughout the whole period of incubation with the drug (TNF + FLICA, CPT + FLICA), and (2) the cultures into which FLICA was added only for the final hour before their termination (TNF → FLICA, CPT → FLICA). It is quite evident that the accumulation of FLICA⁻/PI⁺ cells was markedly reduced in the continuous presence of FLICA, indicating that the transition of cells from the FLICA⁺/PI⁺ to FLICA⁻/PI⁺ was prevented in these cultures (Fig. 2). The process of apoptosis, thus, was halted at the FLICA⁺/PI⁺ stage both in TNF- α and CPT-treated cultures maintained with FLICA.

Continuous exposure to FLICA prevented cell loss in the TNF- α or CPT-treated cultures (Figs. 3, 4). Thus, in the absence of FLICA, ~40% of the cell population was lost after a 24-h exposure to TNF- α . In a parallel experiment, 70% of the cell population was lost in the absence of FLICA, after 48-h exposure to CPT. In the absence of FLICA, cell loss was detected as early as 2 h into the treatment process.

The plots representing cell loss in both TNF- α - and CPT-treated cultures have two distinct slopes revealing different rates of cell disappearance. The rate of cell loss during the initial 6 h (TNF- α) or 8 h (CPT) of treatment was distinctly faster than at later time points. Cell loss was markedly suppressed in the cultures containing FLICA at

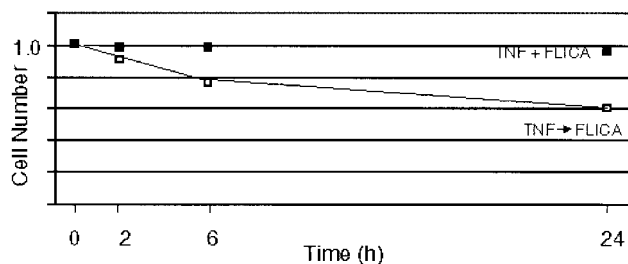


Fig. 3. Cell number in cultures treated at time 0 with TNF- α + CHX and maintained in the absence or presence of FAM-VAD-FMK for up to 24 h. Cultures were treated with TNF- α + CHX alone (TNF- α → FLICA; □) or with TNF- α + CHX plus 20 μ M FAM-VAD-FMK (TNF + FLICA; ■). Cell number in these cultures was periodically measured by hemocytometer. Data are expressed as a fraction of cell number with respect to parallel cultures treated with 20 μ M z-VAD-FMK alone.

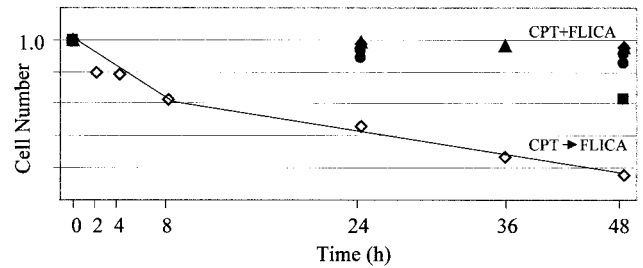


Fig. 4. Cell number in cultures treated at time 0 with CPT and maintained in the absence or presence of FAM-VAD-FMK for up to 18 h. Cultures were treated with CPT alone (CPT → FLICA; ◇) or with CPT plus 10 μ M (■), 20 μ M (●), 30 μ M (◆), or 40 μ M (▲) FAM-VAD-FMK (CPT + FLICA). Cell number in these cultures was periodically measured by hemocytometer. Data are expressed as a fraction of cell number with respect to 0 time control.

10- μ M concentration and was essentially eliminated at the 20- μ M or higher concentration of inhibitor. These data, in conjunction with the results shown in Figure 1, clearly demonstrate that the presence of FLICA in the cultures prevented the disappearance of apoptotic cells by halting apoptosis (stathmo-apoptosis) at the "necrotic stage" (FLICA⁺/PI⁺) prior to loss of cell reactivity with FLICA.

Induction of stathmo-apoptosis allowed us to measure the kinetics of apoptotic cell accumulation during treatment with TNF- α (Fig. 5) or CPT (Fig. 6). The plots representing accumulation of apoptotic cells as a function of treatment time with either TNF- α or CPT each exhibit two distinct slopes revealing different rates of cell transition into apoptosis. Thus, in the TNF- α -treated cultures, about 50% of cells underwent apoptosis during the initial 6 h at an approximate rate of 8% of cells per hour. The remaining cells underwent apoptosis between 6 and 24 h at a rate approximating of 2.5% of cells per hour (Fig. 5). CPT-treated cells also exhibited a ~50% conversion to apoptosis during the initial 8 h at a rate of about of 7%

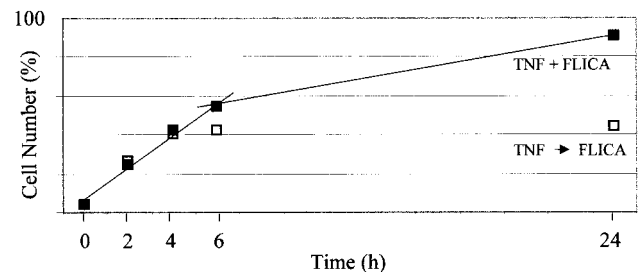


Fig. 5. Kinetics of FAM-VAD-FMK-labeled cell accumulation in cultures treated with TNF- α + CHX and maintained in the absence or presence of FAM-VAD-FMK for up to 24 h. Cultures of HL-60 cells were treated at time 0 with either TNF- α + CHX alone (□) or with TNF- α + CHX plus 20 μ M FAM-VAD-FMK (■). The former cultures (□) were treated with 20 μ M FAM-VAD-FMK during the final hour prior to fluorescence measurement. All cells were exposed to 1 μ g/ml of PI, 5 min before fluorescence measurement. Subpopulations of cells were differentiated on the scattergrams on the basis of differences in intensity of FAM-VAD-FMK (FLICA) and PI-fluorescence, as shown in Figure 1. The percentage of FLICA-positive cells (subpopulations B plus C in Fig. 1) is plotted as a function of time.

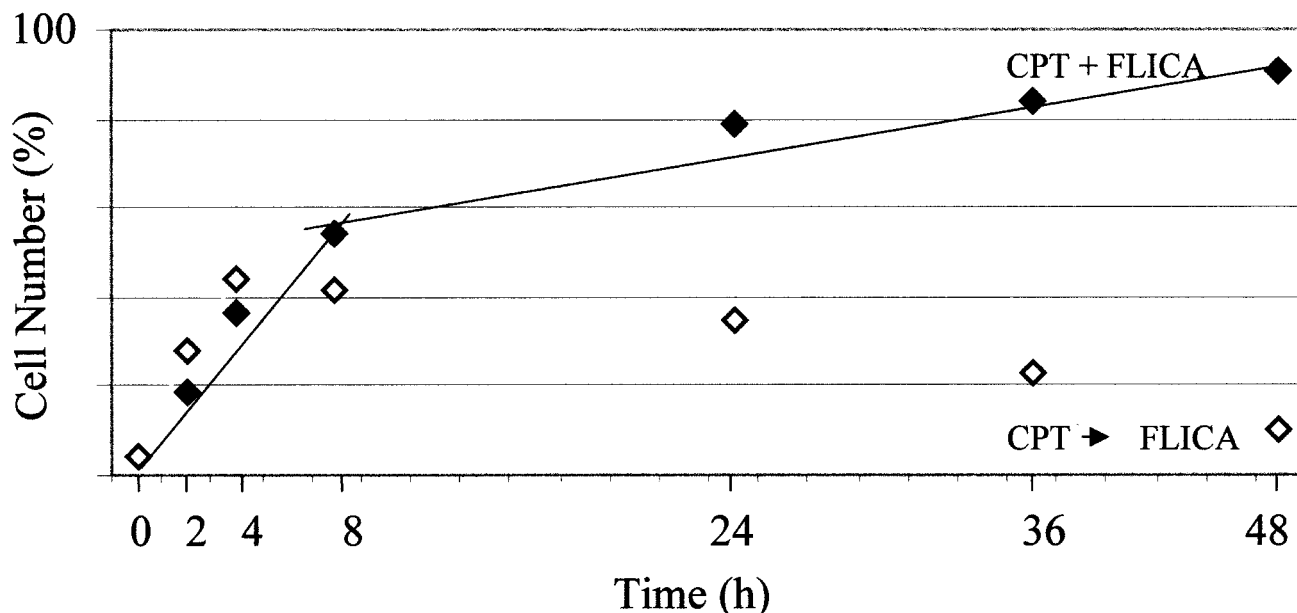


Fig. 6. Kinetics of FAM-VAD-FMK-labeled cell accumulation in cultures treated with CPT and maintained in the absence or presence of FAM-VAD-FMK for up to 48 h. Cultures were treated at time 0 with either CPT alone (CPT → FLICA; \diamond) or with CPT plus 20 μ M FAM-VAD-FMK (CPT + FLICA; \blacklozenge). The former cultures (\diamond) were treated with 20 μ M FAM-VAD-FMK during the final hour prior to fluorescence measurement. All cells were exposed to 1 μ g/ml of PI, 5 min before fluorescence measurement. Subpopulations of cells were differentiated on the scattergrams on the basis of differences in intensity of FAM-VAD-FMK (FLICA)- and PI-fluorescence, as shown in Figure 1. The percentage of FLICA-positive cells (subpopulations B plus C in Fig. 1) is plotted as a function of time.

cells per hour. Remaining cells in this culture were entering apoptosis for up to 48 h at a rate of $\sim 1\%$ of cells per hour (Fig. 6). Control cell cultures exposed to FLICA in the absence of either TNF- α or CPT showed a minor increase in the percentage of FLICA+/PI- (up to 4%) and FLICA+/PI+ (up to 5%) after a 48-h culture period (data not shown). The percent of FLICA-/PI+ cells in this population was very low (less than 1%). This indicates that the rate of spontaneous apoptosis in untreated cell cultures was low, exhibiting an apoptosis conversion rate approximating of 0.2% cells per hour.

We were able to fix the cells that reacted with FLICA, make them permeable, and counterstain their DNA in such a way that unlike in the case of "survival" cell staining (Fig. 1), the intensity of PI fluorescence was in stoichiometric relationship to DNA content (Fig. 7). Because FLICA was covalently attached to the caspase enzymatic centers, the cell-fixation process did not result in the loss of fluorochrome-tagged inhibitor from the cell. The bivariate analysis of cells stained in this manner therefore allowed us to correlate caspase activation with cell-cycle position. Bivariate analysis of cellular DNA content versus FLICA binding performed on cell cultures at the 5-h TNF α + CHX exposure time-point, i.e., when cells were entering apoptosis at a faster rate, is shown in Figure 7. This analysis revealed that cells from all phases of the cell cycle were undergoing apoptosis. There was a selectivity, however, as the proportion of G₁-phase cells among the FLICA-positive cells in TNF- α was higher as compared with the FLICA-negative cell subpopulation. Namely, over

the course of four separate experiments, the mean percentage of G₁ cells within the FLICA-positive cell subpopulation was $16 \pm 5\%$ higher than within FLICA-negative subpopulation. Analysis of the cell cycle of the CPT-

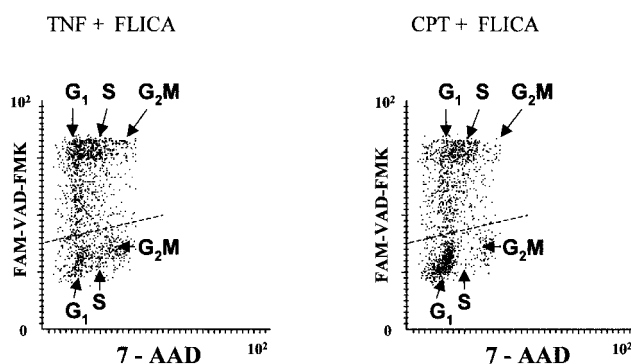


Fig. 7. Scattergrams represent dual fluorescence (FAM-VAD-FMK versus 7-AAD) of HL-60 cells treated with TNF- α + CHX (left) or CPT (right) in the presence of FAM-VAD-FMK for 5 h. Cells were cultured with TNF- α + CHX or CPT, each in continuous presence of 20 μ M FAM-VAD-FMK, subsequently fixed and stained with 7-AAD. The green (FAM-VAD-FMK; maximal pixel) and far red (7-AAD; integral) fluorescence of individual cells was measured by laser scanning cytometry (39,40), as described before (13). The intensity of DNA-associated red fluorescence of 7-AAD allows one to identify cells in G₁, S, and G₂/M, in FLICA-positive (above dashed line) and FLICA-negative (below dashed line) cell subpopulations. Analysis of cell-cycle distribution within these subpopulations revealed predominance of G₁-phase cells entering apoptosis (FLICA-positive) in the TNF- α + CHX-treated culture, consistent with our earlier observations (29,41), and S-phase cells in the CPT-treated culture (see text).

treated cultures revealed that S-phase cells were preferentially undergoing apoptosis during the initial 5 h of treatment: the mean percentage of S-phase cells was 7.6 ± 3.1 fold higher among the FLICA-positive than among the FLICA-negative cells ($n = 4$).

DISCUSSION

Conventional methods, which rely on apoptotic cell enumeration as a means of estimating the AI, are inaccurate regardless of the method of identification. Endpoint analysis fails to take into account the inevitable cell loss due to apoptosis-induced cell disintegration. Indeed, cell loss could be detected as early as 2 or 4 h after administration of TNF- α + CHX or CPT, and was progressive with duration of the treatment. Over 80% of cells were lost in cultures treated with CPT by the 48-h time-point, compared to the time 0 control (Fig. 4). Because apoptotic rather than nonapoptotic cells selectively disappear, the AI is generally underestimated.

A second cause for underestimation of AI is the fact that late apoptotic cells, still present in the cell population, show a loss in their ability to bind FLICA (FLICA-/PI+, subpopulation D, Fig. 1). Methods of identification of apoptotic cells based on the detection of caspase activation, such as those that employ chromogenic or fluorogenic caspase substrates (19–23), assays of PARP cleavage (24,25), or FLICA binding (11–13), are all unable to detect such late apoptotic (necrotic stage) cells.

Estimation of AI can be made unbiased if progression of apoptosis is halted and cell disintegration is prevented. The caspase fluorescent inhibitor FAM-VAD-FMK was adapted for this purpose in the present study. This inhibitor covalently binds to the cysteine of the enzymatic active centers of caspase through the fluoromethyl ketone (FMK) residue forming the thiomethyl ketone (26–28). The binding leads to irreversible inactivation of the enzyme. The three amino-acid (VAD) recognition residue sequence of the inhibitor lacks specificity. This allows FAM-VAD-FMK to bind all caspases, with the possible exception of caspase-2, thus making it the pancaspase inhibitor/marker (28). Because the process of apoptosis was halted at the stage of caspase activation, caspase-mediated events either did not occur in the arrested cell, or did occur but at a much slower rate. Indeed, at 20 μ M and higher concentrations of FAM-VAD-FMK, cells did not disintegrate for up to 48 h (Fig. 3). When examined by microscopy, the arrested cells retained a relatively high-level interference contrast. By flow cytometry, arrested cells exhibited a higher intensity of laser light forward and side scatter signal, compared to the drug-treated cells from cultures lacking FLICA (data not shown). These arrested cells could not, however, exclude PI (Fig. 1) or Trypan blue, and could not be revived when rinsed free of the inhibitor and grown in fresh medium (data not shown).

Arresting cells in apoptosis by the use of FLICA enabled us to plot CAI as a function of time after administration of TNF- α + CHX (Fig. 5) or CPT (Fig. 6) into the cultures. Our data plots revealed the kinetics of cell entry into apoptosis during the treatment process. Two distinct rates

of cell death were apparent for both treatments. The fast rate, when 8% or 7% of cells were undergoing apoptosis per hour, was seen during the initial 6 or 8 h of treatment with TNF- α + CHX or CPT, respectively. Subsequently, cells were dying at a slower rate, with TNF- α + CHX-exposed cells dying at 2.5 times the rate of CPT-exposed cells. In the absence of TNF- α + CHX or CPT, cells were undergoing spontaneous apoptosis at a rate of about 0.2% of cells per hour.

To unveil whether the observed differences in kinetics of cell death may be related to cell-cycle phase, we analyzed the cell-cycle distribution of cells undergoing apoptosis (FLICA-positive cells) at a faster rate, early during treatment (0–5 h), and compared it to nonapoptotic cells of the same cultures (Fig. 7). In the cultures treated with TNF- α , an increase in the proportion of G₁-phase cells among FLICA-positive cells was noticed. This observation is consistent with the increased sensitivity of G₁ cells to TNF- α reported in the literature (29,30). However, because the increase in proportion of G₁ cells among apoptotic compared to nonapoptotic cells was relatively minor (16%), the observed difference in rate of cell death between cells entering rapidly (8% of cells per hour) versus slowly (2.5% of cells per hour) cannot be attributed solely to cell cycle-related differences in sensitivity to TNF- α . It is possible that cell heterogeneity with respect to density of the TNF- α receptors and/or differences in the apoptosis regulatory machinery upstream of the caspases contributed to the difference in the rate of cell death.

In contrast to TNF- α , CPT was much more discriminatory in terms of cell-cycle phase specificity. Namely, in CPT-treated cultures, predominantly S-phase cells were undergoing apoptosis at the faster rate (Fig. 7). This indicates that cells progressing through the S phase were particularly sensitive to CPT, and is consistent with the wealth of published data demonstrating that DNA replicating cells are overly sensitive to DNA topoisomerase I or topoisomerase II inhibitors (31–33). The mechanism of death of these cells involves a collision of DNA replication forks with topoisomerase inhibitor-generated DNA lesions (“cleavable complexes”) (34). Suppression of these collisions, e.g., by inhibitors of DNA replication, prevents apoptosis (32). The slower rate of entrance to apoptosis detected in the 8–48-h CPT-treated cultures may represent the death of G₁ cells that were entering the S phase of the cell cycle.

The stochastic nature of the stathmo-apoptotic plot slopes observed in cells treated with TNF- α + CHX (Fig. 5) as well as CPT (Fig. 6) is consistent with the kinetics of cell progression through the cycle (16). Distributions of the duration of G₁, S, or the overall cell cycle generation time all have a distinct stochastic component (16,35,36). Likewise, distributions of cell sensitivity to a variety of drugs or radiation exposure (survival or clonogenicity curves) all have a characteristic stochastic component (37).

It should be noted that the stathmo-kinetic approach works under an assumption that FAM-VAD-FMK does not affect the kinetics of apoptosis induction. One may ex-

pect, however, that the caspase inhibitor may not only arrest the process of apoptosis, but also may affect induction of apoptosis, *upstream of caspase activation*. In a previous study (11), however, we observed that in cultures continuously treated with CPT, the number of non-apoptotic cells remained similar for up to 48 h, regardless of whether FAM-VAD-FMK was present in the culture all the time or was added during the final hour. The data shown in Figure 1 are consistent with our earlier observation. They also show that in the TNF- α -treated cultures, nearly all cells underwent apoptosis after 24 h, regardless of whether the inhibitor was continuously present or absent. It is unlikely, therefore, that in the case of HL-60 cells treated with CPT or TNF- α , the presence of FAM-VAD-FMK affected *induction* of apoptosis. Controls of this type, however, are needed in every stathmo-kinetic experiment to exclude such a possibility.

It should be noted that the stathmo-apoptosis approach based on the use of FLICA is applicable in analysis of caspase-mediated apoptosis only. Other means of prevention of apoptotic cell disintegration and other means of their detection have to be used to apply this principle in studies of apoptosis that is not caspase-mediated (38).

LITERATURE CITED

- Kerr JFR, Winterford CM, Harmon V. Apoptosis. Its significance in cancer and cancer therapy. *Cancer* 1994;73:2013-2026.
- Majno G, Joris I. Apoptosis, oncosis, and necrosis. An overview of cell death. *Am J Pathol* 1995;146:3-16.
- Vaux DL, Korsmeyer SJ. Cell death in development. *Cell* 1999;96:245-254.
- Strasser A, O'Connor L, Dixit VM. Apoptosis signaling. *Annu Rev Biochem* 2000;69:217-245.
- Darzynkiewicz Z, Bruno S, Del Bino G, Gorczyca W, Hotz MA, Lassota P, Traganos F. Features of apoptotic cells measured by flow cytometry. *Cytometry* 1992;13:795-808.
- Darzynkiewicz Z, Juan G, Li X, Murakami T, Traganos F. Cytometry in cell necrobiology: analysis of apoptosis and accidental cell death (necrosis). *Cytometry* 1997;27:1-20.
- Ormerod MG. The study of apoptotic cells by flow cytometry. *Leukemia* 1998;12:1013-1025.
- Kerr JFR, Wyllie AH, Currie AR. Apoptosis: a basic biological phenomenon with wide-ranging implications in tissue kinetics. *Br J Cancer* 1972;26:239-257.
- Darzynkiewicz Z, Bedner E, Traganos F. Difficulties and pitfalls in analysis of apoptosis. *Methods Cell Biol* 2001;263:527-546.
- Del Bino G, Darzynkiewicz Z, Degraef C, Mosselmans R, Galand P. Comparison of methods based on annexin V binding DNA content or TUNEL for evaluating cell death in HL-60 and adherent MCF-7 cells. *Cell Prolif* 1999;32:25-37.
- Smolewski P, Grabarek J, Phelps DJ, Darzynkiewicz Z. Stathmo-apoptosis: arresting apoptosis by fluorochrome-labeled inhibitor of caspases. *Int J Oncol* 2001;19:657-663.
- Bedner E, Smolewski P, Amstad P, Darzynkiewicz Z. Activation of caspases measured in situ by binding of fluorochrome-labeled inhibitors of caspases (FLICA): correlation with DNA fragmentation. *Exp Cell Res* 2000;260:308-313.
- Smolewski P, Bedner E, Du L, Hsieh T-C, Wu J, Phelps DJ, Darzynkiewicz Z. Detection of caspases activation by fluorochrome-labeled inhibitors: multiparameter analysis by laser scanning cytometry. *Cytometry* 2001;44:73-82.
- Puck TT, Steffen J. Life cycle analysis of mammalian cells. *Biophys J* 1963;3:379-397.
- Tobey RA. Different drugs arrest cells at a number of distinct stages in G₂. *Nature* 1975;254:245-247.
- Darzynkiewicz Z, Traganos F, Kimmel M. Assay of cell cycle kinetics by multivariate flow cytometry using the principle of stathmokinesis. In: Gray JW, Darzynkiewicz Z, editors. *Techniques in cell cycle analysis*. Clifton, NJ: Humana Press; 1997. p 291-336.
- Budihardjo I, Oliver H, Lutter M, Luo X. Biochemical pathways of caspase activation during apoptosis. *Annu Rev Cell Dev Biol* 1999;15:269-290.
- Earnshaw WC, Martins LM, Kaufmann SH. Mammalian caspases: structure, activation, substrates, and functions during apoptosis. *Annu Rev Biochem* 1999;68:383-424.
- Gorman AM, Hirt UA, Zhivotovsky B, Orrenius S, Ceccatelli S. Application of a fluorometric assay to detect caspase activity in thymus tissue undergoing apoptosis *in vivo*. *J Immunol Methods* 1999;226:43-48.
- Liu J, Bhalgat M, Zhang C, Diwu Z, Hoyland B, Klaubert DH. Fluorescent molecular probes V: a sensitive caspase-3 substrate for fluorometric assays. *Bioorg Med Chem Lett* 1999;9:3231-3236.
- Hug H, Los M, Hirt W, Debatin K-M. Rhodamine 110 linked amino acids and peptides as substrates to measure caspase activity upon apoptosis induction in intact cells. *Biochemistry* 1999;9:38:13906-13911.
- Belloc F, Belaund-Rotureau MA, Lavignolle V, Bascans E, Braz-Pereira E, Durrieu F, Lacombe F. Flow cytometry of caspase-3 activation in preapoptotic leukemic cells. *Cytometry* 2000;40:151-160.
- Komoriya A, Packard BZ, Brown MJ, Wu ML, Henkart PA. Assessment of caspase activities in intact apoptotic thymocytes using cell-permeable fluorogenic caspase substrates. *J Exp Med* 2000;191:1819-1828.
- Li X, Darzynkiewicz Z. Cleavage of poly (ADP-ribose) polymerase measured *in situ* in individual cells: relationship to DNA fragmentation and cell cycle position during apoptosis. *Exp Cell Res* 2000;255:125-132.
- Li X, Du L, Darzynkiewicz Z. During apoptosis of HL-60 and U-937 cells caspases are activated independently of dissipation of mitochondrial electrochemical potential. *Exp Cell Res* 2000;257:290-297.
- Thornberry NA, Peterson EP, Zhao JJ, Howard AD, Griffin PR, Chapman KT. Inactivation of interleukin-1 beta converting enzyme by peptide (acyloxy)methyl ketones. *Biochemistry* 1994;33:3934-3940.
- Garcia-Calvo M, Peterson EP, Leiting B, Ruel R, Nicholson DW, Thornberry NA. Inhibition of human caspases by peptide-based and macromolecular inhibitors. *J Biol Chem* 1998;273:32608-32613.
- Thornberry NA, Rano TA, Peterson EP, Rasper DM, Timkey T, Garcia-Calvo M, Houtzager VM, Nordstrom PA, Roy S, Valliancourt JP, Chapman KT, Nicholson DW. A combinatorial approach defines specificities of members of the caspase family and granzyme B. *J Biol Chem* 1997;272:17907-17911.
- Darzynkiewicz Z, Williamson B, Carswell EA, Old LJ. Cell cycle-specific effects of tumor necrosis factor. *Cancer Res* 1984;44:83-90.
- Faraco PR, Ledgerwood EC, Vandenaheele P, Prins JB, Bradley JR. Tumor necrosis factor induces distinct patterns of caspase activation in WEHI-164 cells associated with apoptosis or necrosis depending on cell cycle stage. *Biochem Biophys Res Commun* 1999;261:385-392.
- Del Bino G, Lassota P, Darzynkiewicz Z. The S-phase cytotoxicity of camptothecin. *Exp Cell Res* 1991;193:27-35.
- Deptala A, Li X, Bedner E, Cheng W, Traganos F, Darzynkiewicz Z. Differences in induction of p53, p21^{WAF1} and apoptosis in relation to cell cycle phase of MCF-7 cells treated with camptothecin. *Int J Oncol* 1999;15:861-871.
- Liu W, Zhang R. Upregulation of p21WAF1/CIP1 in human breast cancer cell lines MCF-7 and MDA-MB-468 undergoing apoptosis induced by natural product anticancer drugs 1-hydroxycamptothecin through p53-dependent and independent pathways. *Int J Oncol* 1998;12:793-804.
- Liu LF, Duann P, Lin C-P, D'Arpa P, Wu J. Mechanism of action of camptothecin. *Ann NY Acad Sci* 1996;803:44-49.
- Smith JA, Martin L. Do cells cycle? *Proc Natl Acad Sci USA* 1973;70:1263-1267.
- Darzynkiewicz Z, Crissman H, Traganos F, Steinkamp J. Cell heterogeneity during the cell cycle. *J Cell Physiol* 1982;113:465-474.
- Hill RP, Bush RS. A lung colony assay to determine the radiosensitivity of cells of a solid tumor. *Int J Radiat Biol* 1969;15:435-444.
- Joza N, Susisin SA, Daugas E, Stanford WL, Cho SK, Sasaki T, Elia AJ, Cheng HY, Ravagnan J, Ferri KF, Zamzani N, Wakaham A, Hakem B, Yoshida H, Kong YY, Mak TW, Zuniga-Pflucker JC, Kroemer G, Penninger JM. Essential role of the mitochondrial apoptosis-inducing factor in programmed cell death. *Nature* 2001;410:549-554.
- Kamentsky LA. Laser scanning cytometry. *Methods Cell Biol* 2001;63:51-87.
- Darzynkiewicz Z, Bedner E, Li X, Gorczyca W, Melamed MR. Laser-scanning cytometry: a new instrumentation with many applications. *Exp Cell Res* 1999;249:1-12.
- Darzynkiewicz Z, Carter SP, Old LJ. Effect of recombinant tumor necrosis factor on HL-60 cells. Cell cycle specificity and synergism with actinomycin D. *J Cell Physiol* 1987;130:328-335.